Published in final edited form as:
Biol Chem. 2011 August ; 392(0): 689–697. doi:10.1515/BC.2011.075.

Dynamics of septin ring and collar formation in *Saccharomyces cerevisiae*

Hsin Chen, **Audrey S. Howell**, **Alex Robeson**, and **Daniel J. Lew**[**]
Department of Pharmacology and Cancer Biology, Duke University Medical Center, Durham, NC 27710, USA

Abstract

Although the septin ring and collar in budding yeast were described over 20 years ago, there is still controversy regarding the organization of septin filaments within these structures and about the way in which the ring first forms and about how it converts into a collar at the mother-bud neck. Here we present quantitative analyses of the recruitment of fluorescently-tagged septins to the ring and collar through the cell cycle. Septin ring assembly began several minutes after polarity establishment and this interval was longer in daughter than in mother cells, suggesting asymmetric inheritance of septin regulators. Septins formed an initial faint and irregular ring, which became more regular as septins were recruited at a constant rate. This steady rate of septin recruitment continued for several minutes after the ring converted to a collar at bud emergence. We did not detect a stepwise change in septin fluorescence during the ring-to-collar transition. After collar formation, septins continued to accumulate at the bud neck, though at a reduced rate, until the onset of cytokinesis when the amount of neck-localized septins rapidly decreased. Implications for the mechanism of septin ring assembly are discussed.

Keywords

polarity establishment; septin; yeast

Introduction

The filament-forming septin proteins assemble at various cortical locations in animal and fungal cells, and confer specialized properties on those portions of the plasma membrane (McMurray and Thorner, 2009; Oh and Bi, 2011). Septins were fist described in the budding yeast *Saccharomyces cerevisiae*, where they assemble into distinct ring and hourglass structures as the cells progress through the cell cycle (Figure 1). Yeast septins form stable rod-shaped hetero-octamers in solution, which can polymerize end-to-end to form apolar filaments *in vitro* (Bertin et al., 2008). Electron microscopic observations suggested that septin filaments are highly ordered in the hourglass at the mother-bud neck (Byers and Goetsch, 1976) and polarized fluorescence microscopic observations supported the idea that septins are highly ordered, both in the hourglass and in the rings that flank the cytokinetic furrow (Vrabioiu and Mitchison, 2006). However, the precise arrangements of septin filaments in these structures remain controversial and the organization of septins in the initial ring that forms prior to bud formation remains completely unknown.

[**]Corresponding author: daniel.lew@duke.edu.

Immunofluorescence localization studies suggested that a septin ring of diameter ~1 μm forms suddenly with no discernible intermediates at the site of future bud emergence and that the ring transforms to an hourglass-shaped collar during or immediately after bud emergence (Haarer and Pringle, 1987; Ford and Pringle, 1991; Kim et al., 1991). Fluorescence recovery after photobleaching (FRAP) studies suggested that septins are exchangeable in the ring but 'frozen' and non-exchangeable in the collar (Caviston et al., 2003; Dobbelaere et al., 2003). Confocal microscopy of cells expressing septin-GFP fusions further suggested that a faint fibrous cloud of septins (not seen in fixed-cell images) precedes ring formation at the pre-bud site (Iwase et al., 2006).

Septin-ring assembly is approximately coincident with the clustering of cortical actin patches, which are now known to be sites of ongoing endocytosis (Kaksonen et al., 2006), and with the concentration of Cdc42p, the master regulator of polarity establishment (Ziman et al., 1993), at the presumptive bud site. Septin-ring assembly can proceed without F-actin (Ayscough et al., 1997) but absolutely requires Cdc42p (Iwase et al., 2006) and it is generally accepted that Cdc42p at the polarization site somehow assembles the septin ring around that site.

How does Cdc42p trigger septin ring assembly? The ring surrounds a patch of cortex that carries highly concentrated GTP-Cdc42p. In mutants lacking the Cdc42p effector kinase Cla4p (Cvrckova et al., 1995; Longtine et al., 2000; Gladfelter et al., 2004; Versele and Thorner, 2004) or the Cdc42p-directed GTPase Activating Proteins (GAPs) Rga1p, Rga2p and Bem3p (Gladfelter et al., 2002; Caviston et al., 2003), cells form aberrant rings. Point mutations that slow or accelerate GTP hydrolysis by Cdc42p also impair septin-ring assembly without overtly affecting other functions of Cdc42p (Gladfelter et al., 2002; Caviston et al., 2003). In some cases, the aberrant rings are slightly (*cla4*) or dramatically (*cdc42*^{Y32H}) larger in diameter suggesting that proper Cdc42p signaling (rather than intrinsic septin properties) governs ring diameter (Gladfelter et al., 2002, 2004). These studies indicate that the rate of GTP hydrolysis by Cdc42p is especially important for septin ring assembly.

How does Cdc42p GTP hydrolysis impact septin ring assembly? A trivial explanation would be that excess GTP-Cdc42p interferes with septin assembly. However, this is inconsistent with the recessive nature of the septin defect in the slow-hydrolysis *cdc42* mutants and with the finding that fast-hydrolysis mutants also lead to septin defects (Gladfelter et al., 2002). Moreover, the septin defect can be ameliorated simply by increasing the gene dosage of a slow-hydrolysis *cdc42* mutant (Gladfelter et al., 2002), which would certainly not be the case if excess GTP-Cdc42p were the cause of the defect.

Two speculative hypotheses were put forward regarding the role of Cdc42p in septin ring assembly. One idea is that Cdc42p plays a role analogous to that of the translation elongation factor EF-Tu in protein synthesis (Gladfelter et al., 2002). In this model, complexes containing septins and Cdc42p effectors and/or GAPs would bind GTP-Cdc42p at the polarization site. Proper association with a growing septin ring would trigger hydrolysis of Cdc42p-bound GTP breaking up the complex and leaving a docked septin octamer (or filament) in the growing ring. Improper association would not promote GTP hydrolysis and rather than docking, the intact septin-effector/GAP complex would dissociate from the GTP-Cdc42p and return to the cytoplasm. In this model, Cdc42p GTP hydrolysis is coordinated with septin deposition, accounting for the ill effects of perturbing GTP hydrolysis. However, most details remain unsatisfyingly fuzzy: what does 'proper association' mean? And how would it be coupled to Cdc42p GTP hydrolysis? How would ring formation get started? The analogy to protein elongation leaves the mystery of initiation

unresolved. It is also unclear why the septins would assemble into a ring rather than a patch or some other structure.

The second idea is that Cdc42p acts to catch and release septin octamers/filaments so as to elevate their local concentration at the pre-bud site (Caviston et al., 2003). Sufficiently concentrated septins would then spontaneously self assemble into a ring. GTP-Cdc42p would again bind effector/septin complexes from the cytoplasm and perhaps a coordinated burst of GTP hydrolysis would simultaneously release the septins at high enough local concentration to promote ring assembly. One phenotype seen in some *cdc42* or GAP mutants is a 'cap' of septins at the bud tip and this could be due to effective initial septin recruitment without hydrolysis-stimulated release to form a ring. Again, details of the coupling between septins and Cdc42p GTP hydrolysis remain rather fuzzy and it is not clear why the septins would assemble into a ring.

To better understand the septin ring assembly process, we have re-examined septin assembly at higher temporal resolution than that used previously. We show that septins first appear as a faint irregular ring surrounding the polarization site, approximately 4 min after initial concentration of polarity factors at that site. The amount of septins in the ring then increases gradually for approximately 10 min, until after bud emergence and spreading of the ring to form a collar. Thereafter, septin amount at the collar increases at a reduced rate until cytokinesis and splitting of the septin collar when the septins dissociate from the ring. We discuss the implications of these findings for models of septin ring and collar assembly.

Results

We first wished to examine the timing of septin ring assembly relative to polarity establishment by Cdc42p. Because GFP-Cdc42p is not fully functional (Bi et al., 2000) and we found that both GFP-Cdc42p and a previously described GTP-Cdc42p-binding probe (Tong et al., 2007) altered the polarization process (Howell et al., in preparation), we used Bem1p-GFP (Kozubowski et al., 2008) as a polarity reporter. Bem1p is a polarity scaffold protein that polarizes at the same time as Cdc42p (Howell et al., in preparation). Although many septin fusions carrying fluorescent reporters at the Nor C-termini have been made and all are able to rescue the temperature-sensitive lethality of septin mutants, we found that when combined with various mutations that impair septin organization, the fusions exacerbate the phenotype to a variable degree (data not shown) indicating that they are not fully functional and could therefore perturb the spatiotemporal pattern of septin ring formation. In our strain backgrounds, the least perturbing septin reporters carry GFP or mCherry inserted at residue 13 of Cdc3p (Caviston et al., 2003). Although it is impossible to be sure that the reporters do not affect the process we wish to monitor, selecting the least perturbing reporters and using strains carrying the reporter expressed at the endogenous locus serves to minimize this risk.

Apart from potential effects of fluorescent reporters, the light exposure involved in time-lapse microscopy inflicts significant stress on the cells being filmed (Carlton et al., 2010). We found that cell-cycle progression and particularly the start transition that triggers polarization was delayed or blocked when cells were exposed to too much fluorescent light. We therefore used the low light image acquisition settings in which the kinetics of polarization were unaffected. Image deconvolution of 0.25 μm z-sections was used to increase spatial resolution and we limited time-lapse acquisition to no shorter than 45-s intervals to avoid phototoxicity (this is still considerably faster than previous confocal imaging approaches, Iwase et al., 2006).

In wild-type haploid cells, bud-site-selection rules lead to assembly of new septin rings in the immediate vicinity of old post-cytokinesis septin rings, which can complicate the analysis of assembly dynamics. To circumvent this issue we filmed diploid cells where new rings often form at the opposite end of the cell from the old ring (Chant and Pringle, 1995) and in some experiments we used *rsr1*Δ bud-site-selection mutants in which new rings form at random locations relative to old rings (Bender and Pringle, 1989).

Two-color imaging indicated that septins first began to accumulate at the polarization site 2.25–9 min after Bem1p first accumulated (Figure 2 and Supplementary movie 1). The variability in the timing of septin recruitment was, in large part, due to unexpected differences between mother and daughter cells (Figure 2C and D). In particular, daughter cells almost always had a longer interval between Bem1p polarization and initial septin recruitment (5.93±2.26 min for daughters and 2.80±0.49 min for mothers, n=11). In contrast, the interval between Bem1p polarization and bud emergence was similar in mothers and daughters (Figure 2C).

As suggested previously (Iwase et al., 2006), the septins did not suddenly assemble into a bright ring but rather they accumulated gradually (Figures 2 and 3A). Quantification of the integrated septin ring/collar fluorescence in many cells showed that localized septin content followed three linear phases (Figure 3B).

The first phase, exhibiting the fastest septin assembly rate, began after polarity establishment and lasted for approximately 10 min. Bud emergence occurred during this phase, suggesting that septins were added gradually during septin-ring assembly before bud emergence and continued to be added at the same rate during septin collar formation after bud emergence.

The second phase, exhibiting a 3–4-fold slower septin assembly rate, encompassed most of the budded interval of the cell cycle (40–50 min). The mitotic septin collar was thus significantly (~2-fold) brighter than the collar in small budded cells.

The third phase involved rapid septin disassembly and there appeared to be greater cell-to-cell variability in the rate of this process compared to the rates of initial assembly. In rapidly growing cells such as those filmed here, new septin rings can begin to form before the old rings disassemble, potentially contributing to disassembly.

Returning to the initial assembly process, we exploited the random-budding *rsr1*Δ/*rsr1*Δ bud-site-selection mutants to examine cells in which septin assembly occurred near the top or bottom surface of the cell (Figure 4 and Supplementary movie 2). The earliest visible septin configuration, as seen face on, was in most cases a ring-like shape in which a central ‘hole’ was apparent and fluorescence intensity around the circumference was quite irregular. As the ring became brighter it also became more even, suggesting that septin intercalation filled in gaps in an initially sparse structure.

Discussion

Our analysis of septin dynamics during the cell cycle suggests that septin assembly follows the time course summarized (Figure 5A). A few minutes after initial polarity establishment, septins accumulate gradually in a ring that converts to a collar upon bud emergence. Septins continue to accumulate at the bud neck through most of the cell cycle and (in rapid proliferation conditions) disassemble shortly after cytokinesis. The details of the analysis revealed several surprises in the context of previous ideas about septin assembly.

The first surprise was the variability in the time interval between initial polarity establishment and initial detection of septins at the presumptive bud site (2.25–9 min, Figure 2C). A large part of this variability can be ascribed to mother-daughter differences, with daughters exhibiting a significantly longer lag. Daughters normally have a longer pre-start G1 interval than mothers but this is unlikely to contribute to the observed differences because we are filming cells released from hydroxyurea (HU) arrest (so even daughters are large enough to meet the critical size criteria) and because the interval between Bem1p polarization and bud emergence was similar in mothers and daughters (so other cell-cycle-regulated events do not exhibit the daughter-specific delay). We speculate that asymmetric inheritance of septin regulators by the mother and daughter cells could account for the observed difference in timing. Such differences might arise due to different septin-localized factors being enriched on the mother or bud sides of the collar (Gladfelter et al., 2001) or as a consequence of the regulation of Ace2p and cellular morphogenesis (RAM) network (Weiss et al., 2002; Nelson et al., 2003) or Ash1p (Bobola et al., 1996; Sil and Herskowitz, 1996; Long et al., 1997) asymmetric inheritance pathways.

The second surprise was that initial septin accumulation appeared to occur at a constant rate until a few minutes after bud emergence. This single-phase behavior clashes with the expectation that there would be two distinct assembly events, initial ring formation and ring-to-collar transition, separated by a plateau (mature septin ring) during this interval. However, the conclusion that significant ongoing septin recruitment occurs for several minutes after bud emergence is consistent with EM analyses (Byers and Goetsch, 1976) showing that the number of detectable ‘10 nm filaments’ (now known to depend on septins) increases as the neck diameter expands during initial bud formation. The constant rate of septin accumulation suggests that similar processes could underlie septin recruitment to both the ring and the collar.

A third surprise was that after the collar had formed, septin recruitment continued (albeit at a reduced rate) until mitosis. This slower phase of septin addition could represent a distinct assembly process that differs in kind from that occurring during collar formation or it could represent the continuation of a similar process that is limited simply by the availability of cytoplasmic septin complexes. In the latter view, rapid assembly continues until cytoplasmic septins are exhausted, after which newly synthesized septins are added as they become available. Septin mRNA levels (and presumably therefore synthesis rates) are constant throughout the cell cycle (Spellman et al., 1998; Orlando et al., 2008) and the peak amount of septin fluorescence in the collar is approximately twice that in the initial collar (at the beginning of phase two), consistent with this hypothesis.

Our observations on the kinetics of septin recruitment appear to be at odds with previous reports that there is no recovery of fluorescence after photobleaching of the septin collar (Caviston et al., 2003; Dobbelaere et al., 2003). Because FRAP involves frequent imaging in a confocal using considerably more light than in our wide-field imaging conditions, it seems possible that bleaching during image acquisition could have obscured the continued septin addition to the collar. Moreover, our finding that septins are constantly added to the ring in phase one also calls into question the conclusion drawn from FRAP studies that the septins in the ring are exchangeable (Caviston et al., 2003; Dobbelaere et al., 2003), suggesting the alternative interpretation that recovery of fluorescence after bleaching stems from addition of new septins to the ring.

Two speculative models for septin ring and collar formation, with filaments oriented either parallel (Figure 5B) or perpendicular (Figure 5C) to the mother-bud axis, appear to be consistent with our observations. In these models, the absence of a major reorganization in transitioning from ring to collar naturally accommodates the observation of a single-phase

septin recruitment throughout ring and collar assembly. This would be difficult to account for if the ring and collar had drastically different filament arrangements (e.g., with circumferential filaments in the ring growing at the same rate as axial filaments in the collar and no interruption during the required 90° reorientation).

In (Figure 5B), the initial irregular ring is depicted as a set of ordered but unevenly distributed short filaments surrounding the polarization site (I). Gradual intercalation of more filaments would generate a more intense and regular ring. Upon bud emergence, gradual filament elongation and further intercalation would lead to collar formation (II). Subsequently (III–IV), addition of newly synthesized septins to the edges of the collar continues until cytokinesis, when the septin collar splits (we do not speculate on the orientation of the septin filaments at this stage).

Alternatively, as suggested by an anonymous reviewer and illustrated in Figure 5C, ‘short stretches of discontinuous septin filaments arrayed around the bud neck orthogonal to the mother-bud axis prior to bud emergence (I) could grow in length, as the bud emerges, by the addition of new subunits and eventually coalesce into a number of distinct circumferential hoops (or the gyres of a continuous helical spiral, as suggested by Byers and Goetsch) (II). Growth by addition of septin complexes onto the ends of these initial short segments could occur at multiple locations within the hourglass, depending on the relationship of the ends of these ‘seeds’ with the perimeter of the collar, that is, certain seeds could have ends in the middle of the collar (with respect to the mother-bud axis), allowing for concomitant expansion of the diameter of the septin collar with that of the bud neck via the addition of septin complexes onto the available free ends (III–IV)’.

An attractive feature of Figure 5B is that because the inner edge of the ring grows into the bud while the outer edge remains in the mother, the model naturally accommodates the observation that some septin localized proteins decorate both the inner side of the ring and the bud side of the collar, whereas others decorate both the outer edge of the ring and the mother side of the collar (Kozubowski et al., 2005). Moreover, recent polarized fluorescence microscopy of the ring-to-collar transition suggests that it involves a filament reorientation (Amy Gladfelter, personal communication), which is naturally accommodated by the growth of filaments into the neck along the mother-bud axis as diagrammed (Figure 5B, I–II). These features might be harder to explain in the scenario diagrammed in Figure 5C.

On the other hand, it is relatively easy to imagine the collar expansion constrained by the changing geometry of the plasma membrane (Figure 5C), whereas building a palisade of vertical filaments (Figure 5B) would require an additional mechanism to ensure that the filaments are all of similar length. Moreover, both models leave many important questions unanswered. How does Cdc42p initiate septin ring assembly? Is Cdc42p continuously required for the ongoing septin recruitment to the ring or does it play an initiating role followed by a spontaneous recruitment of septins? Why is septin recruitment so slow: what is the rate-limiting step? Application of the microscopy approaches described here to mutant cells might help to clarify these issues.

Materials and methods

Yeast strains

Yeast strains used in this study are listed (Table 1). Standard media and procedures were used for yeast genetic manipulations. To generate strains expressing Bem1p-GFP, a plasmid (pDLB2968) (Kozubowski et al., 2008) containing a C-terminal fragment of *BEM1* fused to GFP was cut with PstI and transformed to target integration at *BEM1.* Strains expressing

Cdc3p-mCherry or Cdc3p-GFP were constructed by integrating BglII-cut YIp128-CDC3-mCherry or YIp211-CDC3-GFP (Tong et al., 2007) at *CDC3*.

Microscopy

Live cell imaging was performed as previously described (Howell et al., 2009). Exponentially growing cells were mounted on a slide with a slab of complete synthetic medium solidified with 2% agarose (Denville Scientific, Inc.), sealed with Vaseline (Unilever) and filmed at 30°C. With the exception of data in Figure 4 and Supplementary movie 2, cells were synchronized with 200 mM hydroxyurea (HU) (Sigma-Aldrich) in complete synthetic medium (MP Biomedicals) for 3 h at 30°C, washed and released into fresh medium for 1 h and 5 min prior to filming. Synchronization with HU shortens the filming time required to acquire enough septin assembly events for quantification and fortuitously increased cells tolerance of light exposure (Howell et al., in preparation). Images were acquired with an AxioObserver Z1 (Carl Zeiss) with a 100×/1.46 Plan Apochromat oil immersion objective and a QuantEM back-thinned EM-CCD camera (Photometrics). Cells were exposed to 2% neutral-density-filtered excitation light for 250 ms for GFP and 150 ms for RFP during each image acquisition. Timelapse movies were taken either with 30 z-planes at 0.25 μm steps or with 15 z-planes at 0.5 μm steps and displayed as maximum projections. GFP and differential interference contrast (DIC) z-stacks were acquired before RFP z-stacks; a delay of 15–20 s between the two colors is expected.

Image analysis

Images were deconvolved with Huygens Essential software (Scientific Volume Imaging) using the classic maximum likelihood estimation and predicted point-spread function with a background value set constant across all images from the same timelapse, with a signal to noise ratio of 10 and a maximum of 40 iterations. The deconvolved images were compiled with MetaMorph (Molecular Devices) and scored visually for the initial time points of Bem1p-GFP and Cdc3p-mCherry polarization. Images for presentation were processed using MetaMorph and ImageJ (U.S. National Institutes of Health). Quantification of intensity was performed utilizing Volocity (Improvision, Inc.) with a threshold set to select only the polarized signal. The summed intensity was recorded for each timepoint and was plotted using Excel (Microsoft) or Mathematica (Wolfram). The tri-linear fit in Figure 3 was identified by a Mathematica function: FindFit[data_,Piecewise[{{m1 x+b1, x<a1}, {m2 x+(m1−m2) a1+b1, a1<x<a2}, {m3 x+(m2−m3) a2+(m1−m2) a1+b1, a2<x}}, {{a1, 20}, {a2, 50}, m1, m2, m3, {b1, 0}}, x]. Bud emergence was identified as the earliest contrast change (appearance of a white spot in many cases) at the bud site in a DIC timelapse. The image size of Figure 4B was increased by amplifying pixel numbers using Photoshop (Adobe).

Supplementary materials (see www.reference-global.com/toc/bchm/392/8-9)

Supplementary Material

Refer to Web version on PubMed Central for supplementary material.

Acknowledgments

We thank Amy Gladfelter for sharing unpublished information, Nick Buchler and Josh Socolar for help with the tri-linear fits, and Amy Gladfelter and Erfei Bi for stimulating discussions. The authors thank an anonymous referee for suggesting the model to account for our data that is now shown schematically Figure 5C and presented in our Discussion. This work was supported by NIH grant GM53050 to D.J.L.

References

Ayscough KR, Stryker J, Pokala N, Sanders M, Crews P, Drubin DG. High rates of actin filament turnover in budding yeast and roles for actin in establishment and maintenance of cell polarity revealed using the actin inhibitor latrunculin-A. J Cell Biol. 1997; 137:399–416. [PubMed: 9128251]

Bender A, Pringle JR. Multicopy suppression of the cdc24 budding defect in yeast by CDC42 and three newly identified genes including the ras-related gene RSR1. Proc Natl Acad Sci USA. 1989; 86:9976–9980. [PubMed: 2690082]

Bertin A, McMurray MA, Grob P, Park SS, Garcia G 3rd, Patanwala I, Ng HL, Alber T, Thorner J, Nogales E. *Saccharomyces cerevisiae* septins: supramolecular organization of heterooligomers and the mechanism of filament assembly. Proc Natl Acad Sci USA. 2008; 105:8274–8279. [PubMed: 18550837]

Bi E, Chiavetta JB, Chen H, Chen GC, Chan CS, Pringle JR. Identification of novel, evolutionarily conserved Cdc42p-interacting proteins and of redundant pathways linking Cdc24p and Cdc42p to actin polarization in yeast. Mol Biol Cell. 2000; 11:773–793. [PubMed: 10679030]

Bobola N, Jansen RP, Shin TH, Nasmyth K. Asymmetric accumulation of Ash1p in postanaphase nuclei depends on a myosin and restricts yeast mating-type switching to mother cells. Cell. 1996; 84:699–709. [PubMed: 8625408]

Byers B, Goetsch L. A highly ordered ring of membrane-associated filaments in budding yeast. J Cell Biol. 1976; 69:717–721. [PubMed: 773946]

Carlton PM, Boulanger J, Kervrann C, Sibarita JB, Salamero J, Gordon-Messer S, Bressan D, Haber JE, Haase S, Shao L, et al. Fast live simultaneous multiwavelength four-dimensional optical microscopy. Proc Natl Acad Sci USA. 2010; 107:16016–16022. [PubMed: 20705899]

Caviston JP, Longtine M, Pringle JR, Bi E. The role of Cdc42p GTPase-activating proteins in assembly of the septin ring in yeast. Mol Biol Cell. 2003; 14:4051–4066. [PubMed: 14517318]

Chant J, Pringle JR. Patterns of bud-site selection in the yeast *Saccharomyces cerevisiae*. J Cell Biol. 1995; 129:751–765. [PubMed: 7730409]

Cvrckova F, De Virgilio C, Manser E, Pringle JR, Nasmyth K. Ste20-like protein kinases are required for normal localization of cell growth and for cytokinesis in budding yeast. Genes Dev. 1995; 9:1817–1830. [PubMed: 7649470]

Dobbelaere J, Gentry MS, Hallberg RL, Barral Y. Phosphorylation-dependent regulation of septin dynamics during the cell cycle. Dev Cell. 2003; 4:345–357. [PubMed: 12636916]

Ford SK, Pringle JR. Cellular morphogenesis in the *Saccharomyces cerevisiae* cell cycle: localization of the *CDC11* gene product and the timing of events at the budding site. Dev Genet. 1991; 12:281–292. [PubMed: 1934633]

Gladfelter AS, Pringle JR, Lew DJ. The septin cortex at the yeast mother-bud neck. Curr Opin Microbiol. 2001; 4:681–689. [PubMed: 11731320]

Gladfelter AS, Bose I, Zyla TR, Bardes ES, Lew DJ. Septin ring assembly involves cycles of GTP loading and hydrolysis by Cdc42p. J Cell Biol. 2002; 156:315–326. [PubMed: 11807094]

Gladfelter AS, Zyla TR, Lew DJ. Genetic interactions among regulators of septin organization. Eukaryotic Cell. 2004; 3:847–54. [PubMed: 15302817]

Haarer BK, Pringle JR. Immunofluorescence localization of the *Saccharomyces cerevisiae CDC12* gene product to the vicinity of the 10-nm filaments in the mother-bud neck. Mol Cell Biol. 1987; 7:3678–3687. [PubMed: 3316985]

Howell AS, Savage NS, Johnson SA, Bose I, Wagner AW, Zyla TR, Nijhout HF, Reed MC, Goryachev AB, Lew DJ. Singularity in polarization: rewiring yeast cells to make two buds. Cell. 2009; 139:731–743. [PubMed: 19914166]

Iwase M, Luo J, Nagaraj S, Longtine M, Kim HB, Haarer BK, Caruso C, Tong Z, Pringle JR, Bi E. Role of a Cdc42p effector pathway in recruitment of the yeast septins to the presumptive bud site. Mol Biol Cell. 2006; 17:1110–1125. [PubMed: 16371506]

Kaksonen M, Toret CP, Drubin DG. Harnessing actin dynamics for clathrin-mediated endocytosis. Nat Rev Mol Cell Biol. 2006; 7:404–414. [PubMed: 16723976]

Kim HB, Haarer BK, Pringle JR. Cellular morphogenesis in the *Saccharomyces cerevisiae* cell cycle: localization of the *CDC3* gene product and the timing of events at the budding site. J Cell Biol. 1991; 112:535–544. [PubMed: 1993729]

Kozubowski L, Larson JR, Tatchell K. Role of the septin ring in the asymmetric localization of proteins at the mother-bud neck in *Saccharomyces cerevisiae*. Mol Biol Cell. 2005; 16:3455–3466. [PubMed: 15901837]

Kozubowski L, Saito K, Johnson JM, Howell AS, Zyla TR, Lew DJ. Symmetry-breaking polarization driven by a Cdc42p GEF-PAK complex. Curr Biol. 2008; 18:1719–1726. [PubMed: 19013066]

Long RM, Singer RH, Meng X, Gonzalez I, Nasmyth K, Jansen RP. Mating type switching in yeast controlled by asymmetric localization of ASH1 mRNA. Science. 1997; 277:383–387. [PubMed: 9219698]

Longtine MS, Theesfeld CL, McMillan JN, Weaver E, Pringle JR, Lew DJ. Septin-dependent assembly of a cell-cycle-regulatory module in *Saccharomyces cerevisiae*. Mol Cell Biol. 2000; 20:4049–4061. [PubMed: 10805747]

McMurray MA, Thorner J. Septins: molecular partitioning and the generation of cellular asymmetry. Cell Div. 2009; 4:18. [PubMed: 19709431]

Nelson B, Kurischko C, Horecka J, Mody M, Nair P, Pratt L, Zougman A, McBroom LD, Hughes TR, Boone C, et al. RAM: a conserved signaling network that regulates Ace2p transcriptional activity and polarized morphogenesis. Mol Biol Cell. 2003; 14:3782–3803. [PubMed: 12972564]

Oh Y, Bi E. Septin structure and function in yeast and beyond. Trends Cell Biol. 2011; 21:141–148. [PubMed: 21177106]

Orlando DA, Lin CY, Bernard A, Wang JY, Socolar JE, Iversen ES, Hartemink AJ, Haase SB. Global control of cell-cycle transcription by coupled CDK and network oscillators. Nature. 2008; 453:944–947. [PubMed: 18463633]

Sil A, Herskowitz I. Identification of asymmetrically localized determinant, Ash1p, required for lineage-specific transcription of the yeast HO gene. Cell. 1996; 84:711–722. [PubMed: 8625409]

Spellman PT, Sherlock G, Zhang MQ, Iyer VR, Anders K, Eisen MB, Brown PO, Botstein D, Futcher B. Comprehensive identification of cell cycle-regulated genes of the yeast *Saccharomyces cerevisiae* by microarray hybridization. Mol Biol Cell. 1998; 9:3273–3297. [PubMed: 9843569]

Tong Z, Gao XD, Howell AS, Bose I, Lew DJ, Bi E. Adjacent positioning of cellular structures enabled by a Cdc42 GTPase-activating protein-mediated zone of inhibition. J Cell Biol. 2007; 179:1375–1384. [PubMed: 18166650]

Versele M, Thorner J. Septin collar formation in budding yeast requires GTP binding and direct phosphorylation by the PAK, Cla4. J Cell Biol. 2004; 164:701–715. [PubMed: 14993234]

Vrabioiu AM, Mitchison TJ. Structural insights into yeast septin organization from polarized fluorescence microscopy. Nature. 2006; 443:466–469. [PubMed: 17006515]

Weiss EL, Kurischko C, Zhang C, Shokat K, Drubin DG, Luca FC. The *Saccharomyces cerevisiae* Mob2p-Cbk1p kinase complex promotes polarized growth and acts with the mitotic exit network to facilitate daughter cell-specific localization of Ace2p transcription factor. J Cell Biol. 2002; 158:885–900. [PubMed: 12196508]

Ziman M, Preuss D, Mulholland J, O'Brien JM, Botstein D, Johnson DI. Subcellular localization of Cdc42p, a *Saccharomyces cerevisiae* GTP- binding protein involved in the control of cell polarity. Mol Biol Cell. 1993; 4:1307–1316. [PubMed: 8167411]

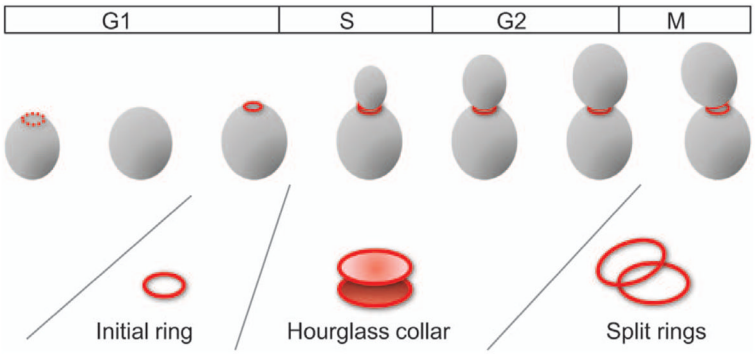

Figure 1. Septin rings and collar through the yeast cell cycle

Cartoon showing initial small ring, hourglass collar and large split rings observed during the yeast cell cycle.

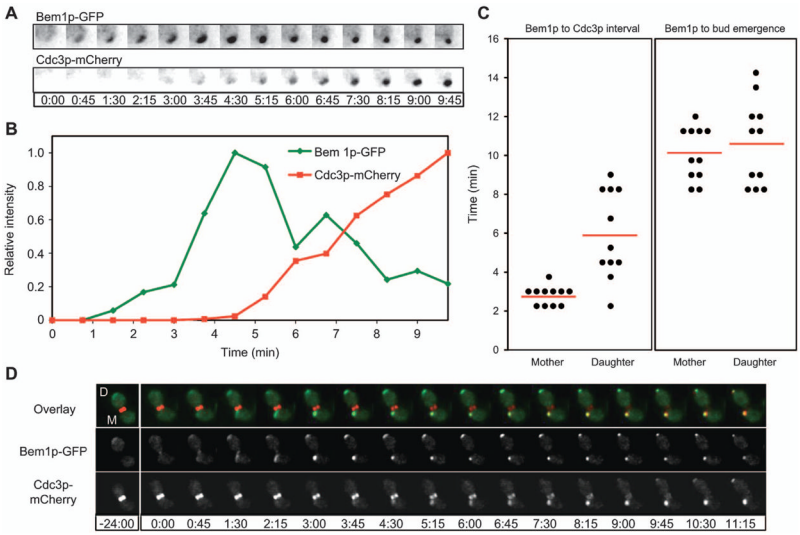

Figure 2. Timing of septin accumulation relative to the polarity marker Bem1p

(A) Illustrative cell from a deconvolved time-lapse movie of strain DLY11909 showing inverted images (so that fluorescent signal appears dark on light background) of Bem1p-GFP and Cdc3p-mCherry. (B) Quantification of Bem1p-GFP and Cdc3p-mCherry intensity for the cell in (A). (C) The interval between initial Bem1p-GFP and initial Cdc3p-mCherry detection was measured for 22 cells, separated into the 11 component mother and daughter cells (left). The interval between initial Bem1p-GFP and initial bud emergence is plotted for the same cells (right). Red lines indicate average intervals in each case. Mothers and daughters were distinguished by noting which cell displayed apical growth (tip localized Bem1p-GFP) in the previous cell cycle (daughter). (D) Illustrative mother-daughter cell. Time is indicated in min:s.

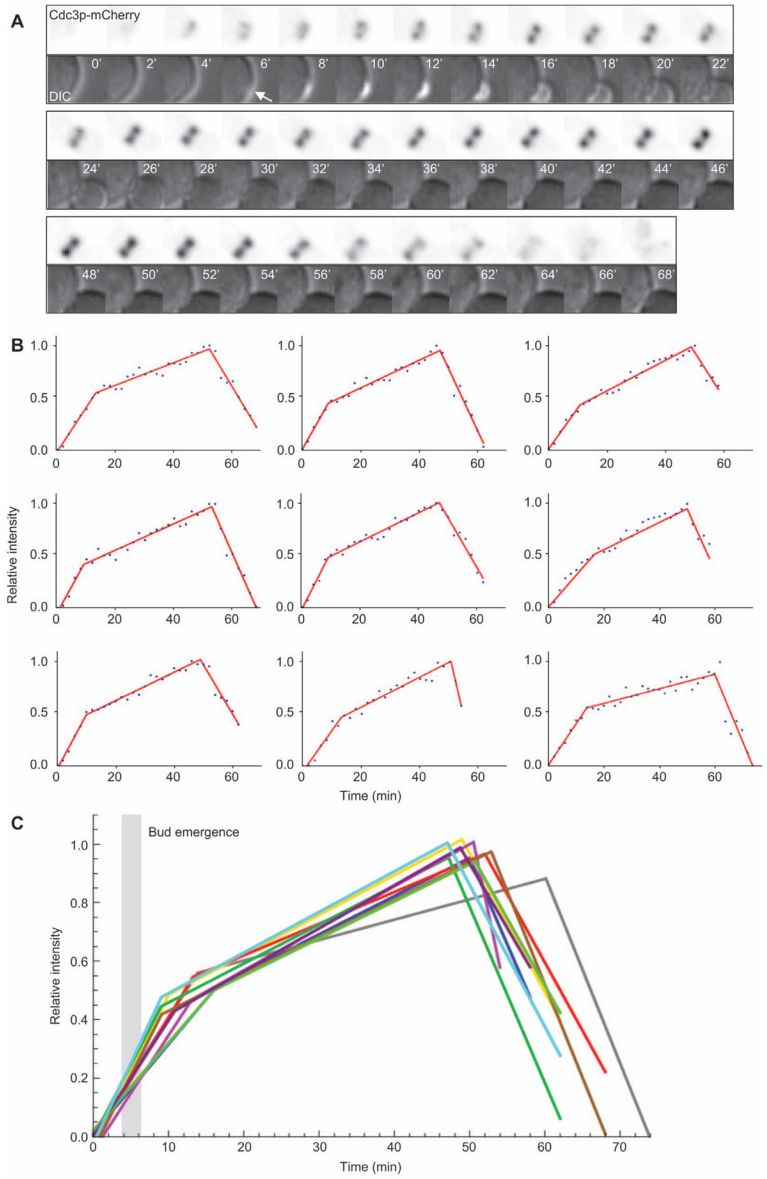

Figure 3. Kinetics of septin accumulation in the ring/collar during the cell cycle

(A) Illustrative cell from a movie of strain DLY13344 showing inverted side-on images of the septin ring/collar. DIC images show timing of bud emergence (indicated by arrow). (B) Quantification of Cdc3p-mCherry intensity in the ring/collar for a panel of nine cells. Datapoints were fit with a tri-linear scheme as described in the Methods (lines). (C) Overlay of the tri-linear fits. Gray bar indicates the time interval during which the cells underwent bud emergence.

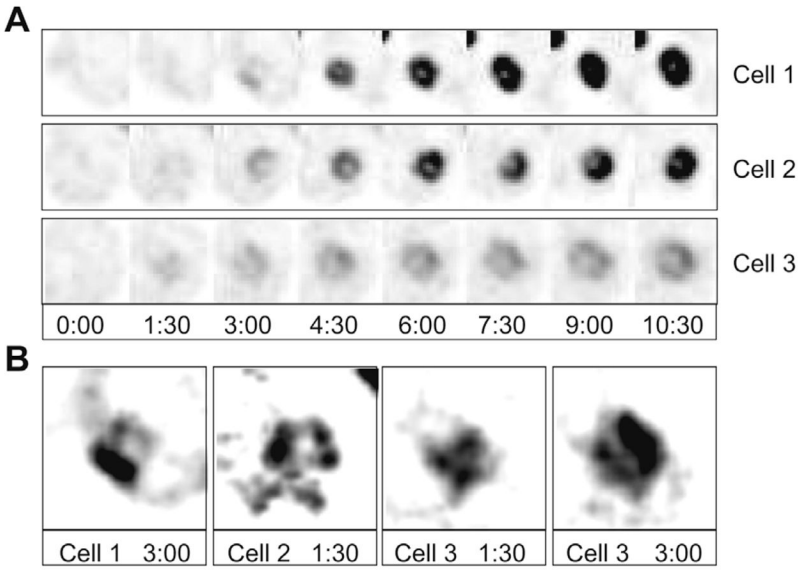

Figure 4. Initial stages of septin ring assembly

(A) Illustrative cells from a movie of strain DLY11784 showing inverted end-on images of septin ring assembly. (B) The earliest timepoints with detectable signal were enlarged and manipulated to increase the signal and reduce the background.

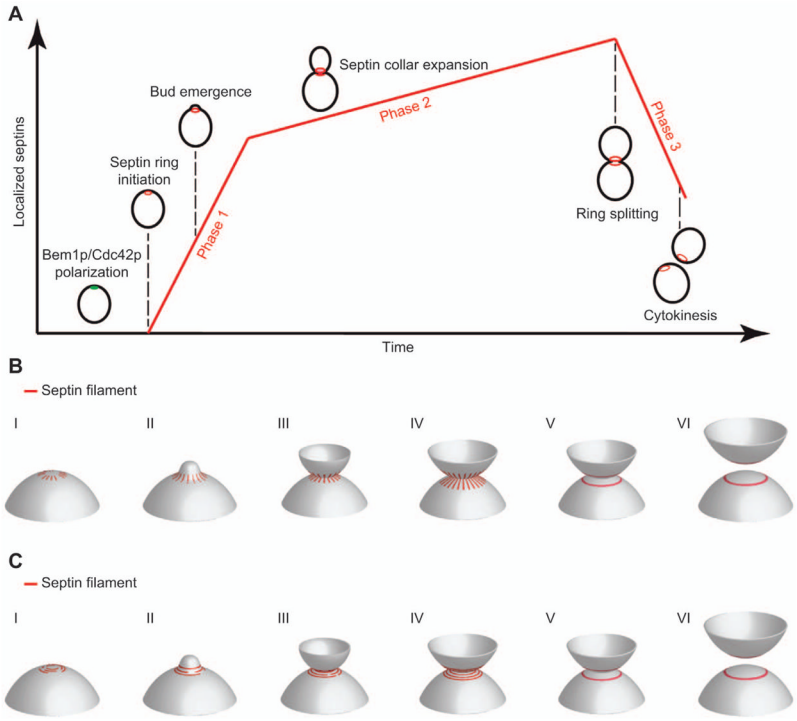

Figure 5. Summary and model for septin ring and collar formation

(A) Summary of septin recruitment during the cell cycle based on fluorescence intensity measurements. Polarity establishment, bud emergence and splitting of the septin collar at the onset of cytokinesis are indicated. (B,C) Speculative models for septin filament assembly and organization. (I) A sparse irregular ring accumulates more septins by intercalation. (II) Bud emergence and continuing septin recruitment until they form an hourglass-shaped collar (III). Slower septin recruitment continues during G2/M (IV) until the collar splits during mitotic exit (V). After cytokinesis, the remnant septin ring (VI) is of larger diameter than the new septin ring that forms in the next cycle (I).

Table 1

Yeast strains used in this study.

Strain	Relevant genotype	Source
DLY11784	**a**/α *ABP1-mCherry:Kan/ABP1-mCherry:Kan rsr1::TRP1/rsr1::TRP1 CDC3-GFP:URA3/CDC3-GFP:URA3*	This study
DLY11909	**a**/α *CDC3-mcherry:LEU2/CDC3-mcherry:LEU2 BEM1-GFP:LEU2/BEM1-GFP:LEU2*	This study
DLY13344	**a**/α *CDC3-mCherry:LEU2/CDC3-mCherry:LEU2 BNR1-GFP:HIS3/BNR1-GFP:HIS3*	This study

All strains are in the YEF473 background (*his3*-Δ*200 leu2*-Δ*1 lys2-801 trp1*-Δ*63 ura3-52*).